Optical Engineering

OpticalEngineering.SPIEDigitalLibrary.org

Nonzero-drift differential all-fiber-optic heterodyne Doppler measurement system

Xiongxing Zhang
Yanping Li
Wei Wang
Haibin Chen
Zilong Guo
Yuxiang Yang

SPIE.

Xiongxing Zhang, Yanping Li, Wei Wang, Haibin Chen, Zilong Guo, Yuxiang Yang, "Nonzero-drift differential all-fiber-optic heterodyne Doppler measurement system," *Opt. Eng.* **58**(5), 056108 (2019), doi: 10.1117/1.OE.58.5.056108.

Nonzero-drift differential all-fiber-optic heterodyne Doppler measurement system

Xiongxing Zhang,[a,b] Yanping Li,[a,b] Wei Wang,[a,b,*] Haibin Chen,[a,b] Zilong Guo,[a,b] and Yuxiang Yang[c]
[a]Xi'an Technological University, School of Optoelectronics Engineering, Xi'an, China
[b]Xi'an Technological University, Shaanxi Province Key Lab of Photoelectric Measurement and Instrument Technology, Xi'an, China
[c]Xi'an University of Technology, School of Mechanical and Precision Instrument Engineering, Xi'an, China

Abstract. To eliminate the serious detrimental effects caused by frequency drifts of acousto-optic frequency shifters (AOFSs) in conventional all-fiber-optic heterodyne Doppler measurement systems, a differential all-fiber-optic heterodyne configuration is proposed. By delicate arrangement of the fiber-optic path and using only one AOFS, zero drift, which commonly occurs in conventional systems, is eliminated. Based on the proposed configuration, a differential all-fiber-optic heterodyne Doppler measurement system has been built. Using a piezoelectric ceramic oscillator as the moving object, it has been verified that the proposed system is able to eliminate zero drift, and the displacement and velocity measurement accuracies reach 0.775 μm and 0.009 mm/s, respectively. It has been shown that the differential all-fiber-optic heterodyne Doppler measurement system can achieve good performance in both displacement and velocity measurements, even in a harsh environment with drastic temperature variation. [DOI: 10.1117/1.OE.58.5.056108]

Keywords: Doppler effect; heterodyne detection; zero drift; all-fiber-optic Doppler measurement.

Paper 190078 received Jan. 31, 2019; accepted for publication Apr. 26, 2019; published online May 21, 2019.

1 Introduction

Laser Doppler measurement is a technique based on the Doppler effect—in this technique, a laser beam is scattered by a moving object; the instantaneous velocity of the object is proportional to the Doppler frequency shift of the laser beam and can be extracted through the interference of the signal and reference beams.[1,2] Laser Doppler measurement offers the advantages of noncontact and high-sensitivity measurement, along with a large operating distance; therefore, it has been widely applied in velocimeters, displacement sensors, vibrometers, accelerometers, hydrophones, etc.[3–7] However, the conventional laser Doppler measurement system commonly uses discrete optical elements and devices, which makes the system large, complex, difficult to align, and susceptible to vibration interference, and in particular, unsuitable for deployment in confined or restricted areas. Owing to the rapid development of fiber technology, using fiber-optic-type devices, all-fiber-optic Doppler measurement systems can be constructed, which are more compact, versatile, and convenient to use in various environments.[8–13]

All laser Doppler measurement systems are based on the interference of light. All-fiber-optic laser Doppler measurement systems can be classified into two types of interferometric configurations according to the detection method used: homodyne and heterodyne interferometries.[14,15] The homodyne interferometric configuration for an all-fiber-optic Doppler measurement system is simple, but if the direction of motion of an object needs to be determined, the system becomes very complicated.[14] For the heterodyne interferometric configuration, a known frequency shift can be added to the signal or reference beam, and from the beat frequency of the two beams, both the magnitude and the direction of the velocity can be extracted directly. Compared with the homodyne configuration, heterodyne Doppler measurement systems offer much higher sensitivity and accuracy and much stronger anti-interference ability.[16,17]

In all-fiber-optic heterodyne Doppler measurement systems, acousto-optic frequency shifters (AOFSs) are commonly used to achieve the frequency shift of the signal or reference beam.[15,17–21] AOFSs offer low insertion loss, high extinction ratio, fast response, and relatively high-frequency stability and are compatible with fiber-optic paths. However, in real conditions, AOFSs suffer from frequency shift fluctuations and drifts. The random frequency shift fluctuations will directly determine the minimum resolvable Doppler frequency shift, and the accuracy and resolution of velocity or displacement measurement. Several studies have been conducted on accuracy or resolution improvement of all-fiber-optic heterodyne Doppler measurement systems.[19,21–23] The drift in the frequency shift of an AOFS is primarily a result of the frequency drift of the driving signal and influences the accurate determination of the Doppler frequency shift caused by the moving object, which will also severely reduce deterioration of the performance of all-fiber-optic heterodyne Doppler measurement systems. For displacement measurement, the drift in the frequency shift will lead to a cumulative error during the measurement process, because displacement is obtained by integrating velocity, and errors caused by velocity deviation due to the inaccurate determination of the Doppler frequency shift will be continuously accumulated. Furthermore, even in velocity measurement, the drift in the frequency shift will lead to a measurement deviation; this is because, in a heterodyne system, the velocity is calculated from the Doppler frequency, which is obtained by subtracting the AOFS's nominal frequency shift from the frequency of the interference signal and the frequency shift

*Address all correspondence Wei Wang, E-mail: wangwei@xatu.edu.cn

of the AOFS involves time-varying drifts. The effect of drift in the frequency shifts on the all-fiber-optic heterodyne Doppler measurement is called zero drift here.

To improve the performance of all-fiber-optic heterodyne Doppler measurement systems, the zero drift caused by the drift in the frequency shift from the AOFS should be precisely eliminated. Shang et al.[19] proposed a method based on the subtraction of the electric driving signal's frequency of the AOFS from the interferometric signal's frequency to eliminate the frequency drift of AOFS. However, there existed a time delay between the interferometric and the driving signals, and as a result, the zero drift cannot be completely eliminated. The reported displacement and velocity measuring uncertainties were <4.6% and 4.14%, respectively, and the minimal resolvable velocity was about 96.9 nm/s. Another method proposed involves offsetting the frequency drift by simultaneously using two or more AOFSs to form two or more Mach–Zehnder interferometers; through differential treatment of two or more interferometric signals, the drift in the frequency shift of the AOFS can be effectively eliminated.[23] Shirai et al.[21] presented a method to perform velocity measurements of a turbulent channel flow; this method removes the drift in the frequency shift by employing three AOFSs to achieve frequency shifts of 120, 80, and 60 MHz. They achieved a relative velocity accuracy of 0.16% and a minimal detectable velocity of <0.1 m/s. Among the existing methods of zero-drift elimination for all-fiber-optic heterodyne Doppler measurements, the method using two or more AOFSs can only eliminate those caused by the instability of AOFS's driving signal and involved complicated and expensive configurations. Furthermore, the frequency inconsistency of the clocks of the photoelectric detection circuit and the AOFS driving circuit can introduce zero drift even if the AOFS is accurately frequency shifted.

In this paper, we propose a configuration of an all-fiber-optic heterodyne Doppler measurement system that includes two Mach–Zehnder interferometers using only one AOFS, which can synchronously obtain AOFS frequency shift and the sum of Doppler and AOFS frequency shifts; through differential treatment of the two interferometric signals obtained by the two interferometers, the measurement performance can be effectively improved. In addition, we experimentally test the system's ability to eliminate the zero drift in heterodyne Doppler displacement and velocity measurements.

2 Typical All-Fiber-Optic Heterodyne Doppler Measurement System

A typical all-fiber-optic heterodyne Doppler measurement system is composed of a fiber-pigtailed distributed feedback (DFB) laser, an optical isolator, two 1×2 couplers, an AOFS, an optical circulator, a fiber collimator, and a photodetector, as shown in Fig. 1. A laser beam emitted by the DFB laser passes through the isolator and then propagates to the 1×2 optical coupler 1; the beam is equally split into two beams. One beam passes through the AOFS and is frequency-shifted as the reference beam; the other beam is coupled into port 1 of the optical circulator and then output from port 2 to the fiber collimator, to be coupled out as a collimated beam incident on the surface of the moving object. The reflected light is frequency-shifted by the Doppler effect and is returned to port 2 of the optical circulator, and then output from port 3 as the signal beam. The two beams coherently interfere through the 1×2 coupler 2 and form a beat frequency signal containing both the Doppler and the AOFS frequency shifts; this signal is finally received by the photodetector.

In the all-fiber-optic heterodyne Doppler measurement system, the reference beam can be expressed as

$$E_A(t) = A_a \cos[2\pi(f_0 + f_A)t + \varphi_1], \tag{1}$$

where A_a is the signal amplitude, f_0 is the laser frequency, f_A is the AOFS frequency shift, and φ_1 is the initial phase of the reference beam.

The signal beam can be expressed as

$$E_D(t) = A_d \cos[2\pi(f_0 + f_D)t + \varphi_2], \tag{2}$$

where A_d is the signal amplitude, f_D is the Doppler frequency shift, and φ_2 is the initial phase of the signal beam.

The Doppler frequency shift f_D can be written as

$$f_D = \frac{2v}{\lambda 0} \cos\theta, \tag{3}$$

where v is the velocity of the object, λ_0 is the laser wavelength, and θ is the angle between the direction of motion of the object and the optical axis. It can be seen that the Doppler frequency shift f_D is proportional to the velocity of the object, which is used to extract the motion parameters of the object in real time.

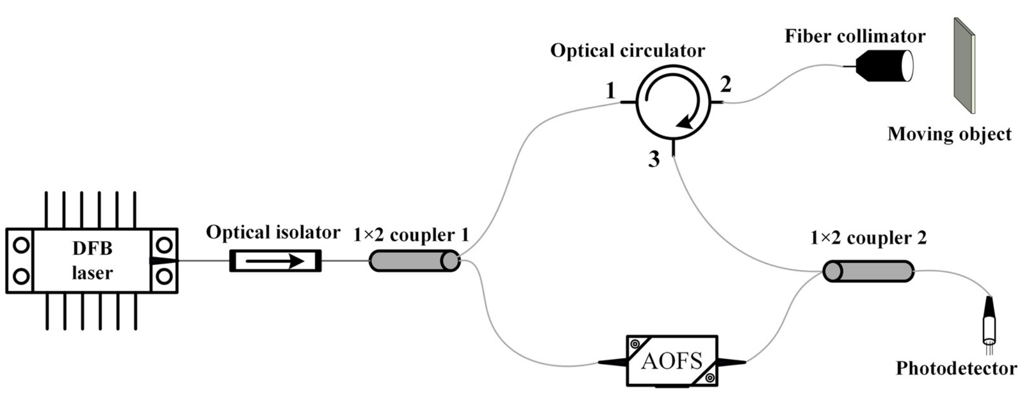

Fig. 1 Schematic representation of a typical all-fiber-optic heterodyne Doppler measurement system.

If the laser beam is incident parallel to the velocity of the moving object, then the velocity can be written as

$$v = \frac{\lambda 0}{2} f_D. \tag{4}$$

The displacement of the moving object can be expressed as

$$s(t) = \int_0^t \frac{\lambda 0}{2} f_D d\tau = \frac{\lambda 0}{2} N(t), \tag{5}$$

where $N(t)$ is the total number of periods counted at time t; therefore, the displacement at any time $s(t)$ can be calculated through a period-counting method.

According to the principle of heterodyne interference, the intensity of the interferometric signal can be expressed as

$$\begin{aligned} I_1(t) = {} & A_a^2 \cos^2[2\pi(f_0 + f_A)t + \varphi_1] \\ & + A_d^2 \cos^2[2\pi(f_0 + f_D)t + \varphi_2] \\ & + A_a A_d \cos[2\pi(2f_0 + f_A + f_D)t + (\varphi_1 + \varphi_2)] \\ & + A_a A_d \cos[2\pi(2f_0 + f_A + f_D)t + (\varphi_1 + \varphi_2)]. \end{aligned} \tag{6}$$

Since the response rate of the photodetector, commonly less than several tens of gigahertz, is far below the optical frequency of the laser, the first three high-frequency terms in the formula will be averaged as a constant photocurrent output; only the signal corresponding to the fourth beat-frequency term can be detected. Therefore, the output photocurrent of the photodetector can be expressed as

$$i = k\left\{\frac{A_a^2 + A_d^2}{2} + A_a A_d \cos[2\pi(f_A - f_D)t + (\varphi_1 - \varphi_2)]\right\}, \tag{7}$$

where k is the sensitivity of the photodetector. By measuring the beat frequency $f = f_A - f_D$, the Doppler frequency shift $f_D = f_A - f$ can be determined easily, and the velocity and displacement of the object can be obtained from Eq. (4) and Eq. (5), respectively.

However, if the AOFS has a frequency drift of Δf_A, then the Doppler frequency shift determined will deviate from f_D, a frequency of Δf_A, as a result, a velocity measurement error of

$$\Delta v = \frac{\lambda_0}{2} \Delta f_A, \tag{8}$$

and a displacement measurement error of

$$\Delta s = \frac{\lambda 0}{2} \int_0^t \Delta f_A d\tau, \tag{9}$$

will be introduced into the Doppler measurement.

It can be seen that the zero drift of the all-fiber-optic heterodyne Doppler measurement system can seriously influence the accurate determination of velocity and displacement.

3 Differential All-Fiber-Optic Heterodyne Doppler Measurement System

To improve the all-fiber-optic heterodyne Doppler measurement, a differential all-fiber-optic heterodyne Doppler measurement system containing two Mach–Zehnder interferometers using only one AOFS is proposed, which is composed of a fiber-pigtailed DFB laser, an optical isolator, a 1×3 coupler, three 1×2 couplers, an AOFS, an optical circulator, a fiber collimator, and two photodetectors, as shown in Fig. 2. The fiber lengths of the fiber optic paths from 1×2 coupler 1 to 1×2 couplers 2 and 3 are equal, and those from 1×2 couplers 2 and 3 to photodetectors 1 and 2, respectively, are equal; this is done to ensure an optical path difference (OPD) of zero. A laser beam emitted by the DFB laser is coupled into the 1×3 optical coupler through the optical isolator. One output beam propagates to port 1 of the optical circulator, incident on the surface of the moving object through port 2 of the optical circulator and the fiber collimator, which is the signal beam E_D and is in the same form as given in Eq. (2). The second beam is frequency-shifted through the AOFS and is equally divided by the 1×2 coupler 1 into two beams, which are the AOFS frequency-shifted reference beams E_A; these are in the same form as given in Eq. (1). One of the reference beams is mixed with the

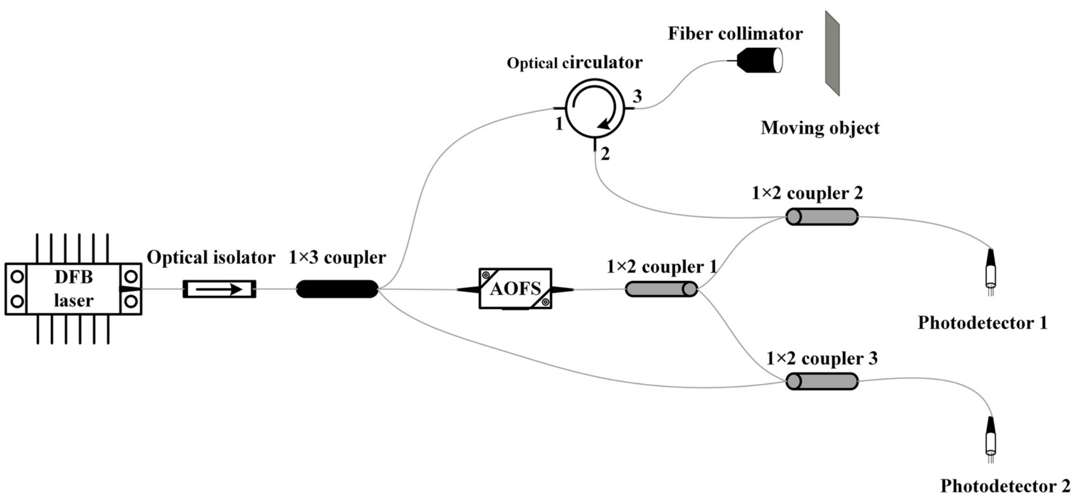

Fig. 2 Schematic representation of the differential all-fiber-optic heterodyne Doppler measurement system without zero drift.

reflected signal beam through 1×2 coupler 2 and is detected by the photodetector 1 to obtain the first interferometric signal, which can be expressed as

$$i_1 = k\left\{\frac{A_a^2 + A_d^2}{2} + A_a A_d \cos[2\pi(f_A - f_D)t + (\varphi_1 - \varphi_2)]\right\}. \tag{10}$$

The third beam output from the 1×3 coupler does not have any frequency shift, which can be called the intrinsic beam E_0 and expressed as

$$E_0(t) = A_0 \cos(2\pi f_0 t + \varphi_0), \tag{11}$$

where f_0 is the original laser frequency of the intrinsic beam. The other part of the reference beam output from 1×2 coupler 1 is mixed with the intrinsic beam through 1×2 coupler 3 and is received by the photodetector 2 to obtain the second interferometric signal, which can be expressed as

$$i_2 = k\left\{\frac{A_0^2 + A_d^2}{2} + A_0 A_d \cos[2\pi f_A t + (\varphi_1 - \varphi_0)]\right\}. \tag{12}$$

Owing to the two beams divided by 1×2 coupler 1 having the same optical characteristics and the zero OPD of the fiber-optic paths from 1×2 coupler 1 to photodetectors 1 and 2, the two interferometric signals can be detected synchronously. The first and second interferometric signals have the same drift in the frequency shift. After photoelectric conversion, by sampling the two interferometric signals simultaneously with the same clock system, measuring and differencing the frequencies of the two signals, the zero drift of the heterodyne Doppler measurement systems caused by the drift in the frequency shift of the AOFS can be completely eliminated; additionally, there are no concerns with inconsistency of the clock systems of the photoelectric detection circuit and the AOFS driving circuit, owing to the differential operation of the two interferometric signals in our differential all-fiber-optic heterodyne Doppler measurement system.

4 Experiments and Discussion

To evaluate the performance of the proposed differential all-fiber-optic heterodyne Doppler measurement system, an experimental setup was built according to the schematic in Fig. 2, as shown in Fig. 3. The DFB laser has a center wavelength of 1550 nm, maximum output power of 20 mW, and linewidth of 3 MHz. The AOFS used was manufactured by Gooch & Housego, UK; the central frequency of the radio frequency driving signal is 40 MHz, the frequency stability of the AOFS is $\pm 0.05\%$, and the frequency shift error is ± 20 kHz. The InGaAs photodiode has a response time of 3.5 ps and a sensitivity of 0.65 A/W. A custom-designed and custom-built signal-processing circuit is used to obtain the two interferometric signals of the two Mach–Zehnder interferometers simultaneously, to completely eliminate the drift in the frequency shift of the AOFS through measuring and differentiating the frequencies of the two signals, and to extract velocity and displacement of the object from the Doppler frequency shift without zero drift.

A piezoelectric ceramic oscillator driven by an open loop piezocontroller was used as the moving object to be

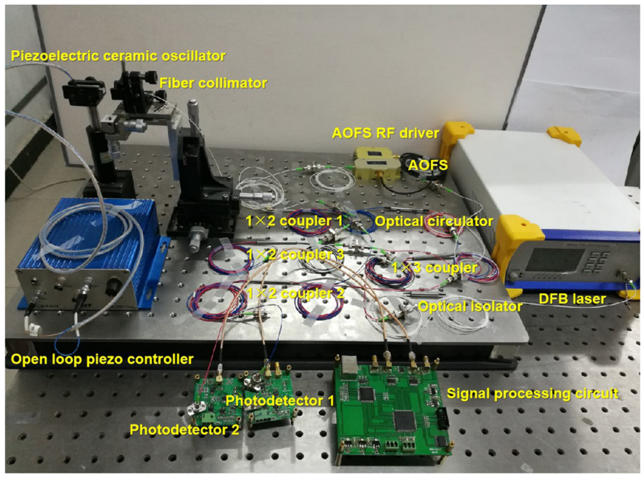

Fig. 3 Experimental setup of the differential all-fiber-optic heterodyne laser Doppler measurement system.

measured using our differential all-fiber-optic heterodyne Doppler measurement system. The piezoelectric ceramic oscillator having a travel range of 18.4 μm, a displacement resolution of 20 nm, and an oscillating frequency of ≤ 60 Hz was fixed on a mechanical holder. The fiber collimator of the differential all-fiber-optic heterodyne Doppler measurement system was fixed on a five-axis precision translation stage. Through careful manual tuning, the laser beam output from the fiber beam was adjusted to be normally incident on the front surface of the piezoelectric ceramic oscillator to achieve a maximal contrast of the interferometric signal on photodetector 1. Since the front surface of the piezoelectric ceramic oscillator was perpendicular to the oscillating direction, the beam direction with the maximal contrast was assumed to be the optimal direction parallel to the moving velocity.

First, the piezoelectric ceramic oscillator is set to operate in a static state. The measurement results are shown in Fig. 4. It can be seen that the measured displacement maintains a value of zero, and the maximum jump of the value is ± 0.775 μm, which is half of the central wavelength of the DFB laser and is much better than those obtained by a conventional fiber-optic heterodyne laser Doppler measurement system with a configuration shown in Fig. 1. During a measurement with a duration of 8 min, due to the AOFS drift in the frequency shift and clock system inconsistency of the photoelectric detection circuit and the AOFS driving circuit, the displacement obtained with the conventional configuration drifted with time. The maximal drift of the displacement measurement had reached a value of 20 μm. A comparison shows that our differential all-fiber-optic heterodyne Doppler measurement system can precisely eliminate zero drift of displacement measurement of the conventional configuration and significantly improve the minimum detectable displacement to half of the wavelength.

Then, the piezoelectric ceramic oscillator is driven by a sinusoidal signal; it undergoes harmonic motion with an oscillating frequency of 50 Hz, and peak-peak values of 4.0, 6.5, 8.0, 9.5, 11.0, 12.5, and 14.0 μm, respectively; the measured results of displacement of our differential all-fiber-optic heterodyne Doppler measurement system are shown in Fig. 5. The displacement curves are consistent with the

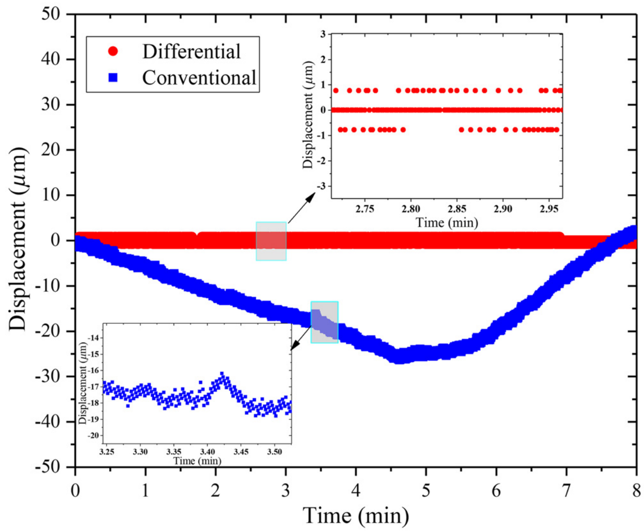

Fig. 4 Displacement measurement of a piezoelectric ceramic oscillator in a static state using the differential all-fiber-optic heterodyne Doppler measurement system (red circle dot); for comparison, the measurement result obtained with a conventional configuration is also shown (blue square dot).

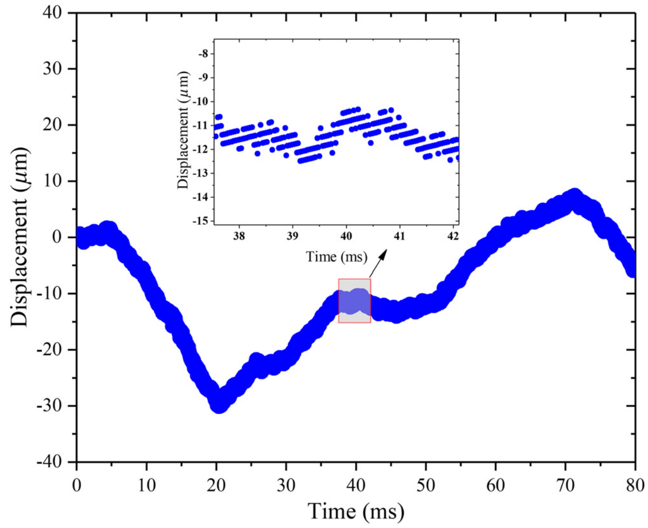

Fig. 6 Displacement measurement results of a piezoelectric ceramic oscillator undergoing harmonic motion with a frequency of 50 Hz and an amplitude of 7.0 μm using a conventional fiber-optic heterodyne laser Doppler measurement system.

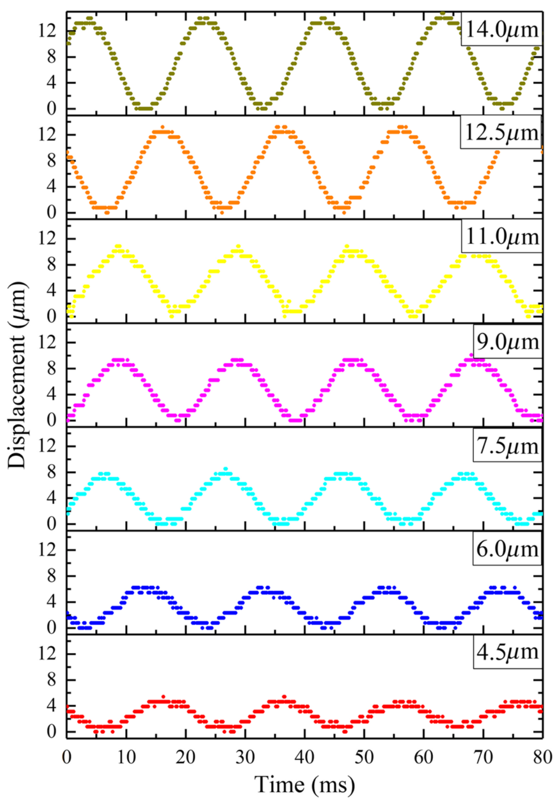

Fig. 5 Displacement measurement results of a piezoelectric ceramic oscillator undergoing harmonic motion with a constant frequency of 50 Hz and various amplitudes using the differential all-fiber-optic heterodyne Doppler measurement system.

predetermined motion of the piezoelectric ceramic oscillator. Compared with the displacement calculated from the displacement–voltage relationship, it can be found that the measurement error is less than the measurement resolution of 0.775 μm, which is substantially lower than the measurement error caused by the zero drift of the conventional configuration.

It should be mentioned that the displacement measurement resolution of 0.775 μm is caused by the period counting algorithm, according to Eq. (5) used in the displacement calculation, which is not a fundamental limit of the method. By the using of a more advanced phase discrimination method, the measurement resolution can be further improved.

We have also attempted to measure the displacement of the piezoelectric ceramic oscillator by using the conventional all-fiber-optic heterodyne Doppler measurement configuration. With a driving frequency of 50 Hz and a maximum driving voltage of 75 V, the piezoelectric ceramic oscillator undergoes harmonic motion with a large amplitude of 7.0 μm, but as Fig. 6 shows, no obvious harmonic motion is observed.

The drift in the frequency shift of AOFS is ± 20 kHz, and the corresponding velocity drift is 15 mm/s. The absolute velocity of the piezoelectric ceramic oscillator is 0 to 2.198 mm/s, which is substantially lower than the velocity drift caused by the AOFS drift in the frequency shift. The Doppler frequency shift caused by the moving piezoelectric ceramic oscillator is considerably less than the drift in the frequency shift of the AOFS to be extracted; this seems to be the reason why we cannot observe the motion form of the piezoelectric ceramic oscillator by using the conventional all-fiber-optic heterodyne Doppler measurement configuration. By comparing the two experimental results, it can be seen that by using the differential all-fiber-optic heterodyne laser Doppler measurement configuration to eliminate the zero drift, the minimum detectable displacement of the all-fiber-optic heterodyne Doppler measurement system can be effectively improved.

To further demonstrate the performance of the differential all-fiber-optic heterodyne Doppler measurement system, we attempted to heat the signal-processing circuit by fan blowing hot air at 200°C with a distance of about 10 cm for >8 min to simulate an environment with drastic temperature variation. The piezoelectric ceramic oscillator was set to operate in a static state again, and the displacement of the

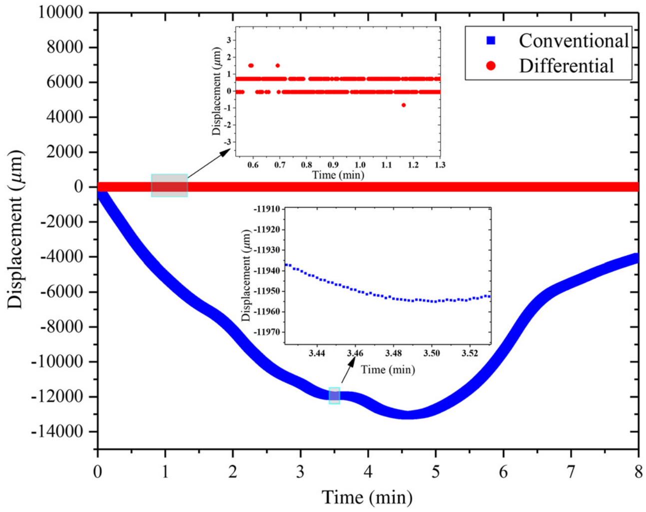

Fig. 7 Displacement measurement of a piezoelectric ceramic oscillator in a static state under an environment with drastic temperature variation using the differential all-fiber-optic heterodyne Doppler measurement system (red circle dot); for comparison, the measurement results obtained by a conventional configuration are also shown (blue square dot).

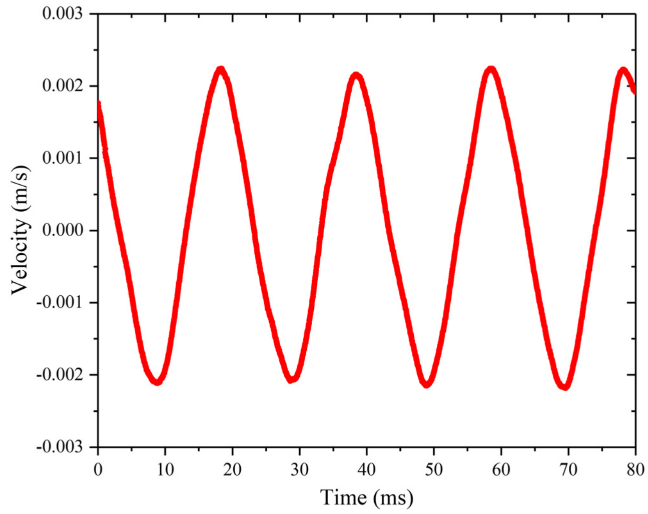

Fig. 8 Velocity of the piezoelectric ceramic oscillator measured using the differential all-fiber-optic heterodyne Doppler measurement system; the piezoelectric ceramic oscillator underwent harmonic motion with a frequency of 50 Hz and displacement amplitude of 7.0 μm.

piezoelectric ceramic oscillator was monitored through our differential all-fiber-optic heterodyne Doppler measurement system. It was found that the displacement drifted in a range from -1.55 to 1.55 μm, as shown in Fig. 7. Compared with the result obtained under normal condition, the zero drift deteriorated slightly. For the displacement measured with the conventional configuration (the electronic circuit hardware was the same, except only one photodetector was used), the displacement drift for the measurement of a static piezoelectric ceramic oscillator reached an unacceptable value of 13 mm; therefore, a conventional all-fiber-optic heterodyne Doppler measurement system cannot withstand drastic temperature variation. However, our differential all-fiber-optic heterodyne Doppler measurement system can still achieve a relatively good accuracy of displacement measurement for the elimination of zero drift, and hence the proposed system showed a strong environmental adaptability.

The differential all-fiber-optic heterodyne Doppler measurement system is also used for velocity measurement. The piezoelectric ceramic oscillator is set to undergo harmonic motion with a frequency of 50 Hz and a displacement amplitude of 7.0 μm. If the displacement of the harmonically moving piezoelectric ceramic oscillator is described by $s(t) = A\cos(\omega t + \varphi_0)$, where A is the displacement amplitude, ω is the angular frequency, φ_0 is the initial phase, then the velocity at any time is $v(t) = -A\omega\cos(\omega t + \varphi_0)$. So, the relationship of the velocity versus time is also in a cosinusoidal form. For a frequency of 50 Hz and a displacement amplitude of 7.0 μm, the velocity range is calculated to be from -2.199 to 2.199 mm. The velocity measured by our system, as shown in Fig. 8, varies sinusoidally with time, ranging from -2.190 to 2.195 mm/s. Therefore, the maximal measurement error in the measurement range is $\sim$0.009 mm/s. Conversely, the conventional all-fiber-optic heterodyne Doppler measurement configuration failed to extract the velocity of the piezoelectric ceramic oscillator. The resolving ability of the differential all-fiber-optic heterodyne Doppler measurement system for a relatively low velocity is achieved through the precise elimination of the zero drift caused by the AOFS drift in the frequency shift and the clock inconsistency of the photoelectric detection and AOFS driving circuits.

5 Conclusions

We proposed a differential all-fiber-optic heterodyne Doppler measurement system to eliminate the zero drift to improve the measurement accuracy and the minimum detectability of displacement or velocity through the well-known Doppler effect. Through careful design of two Mach–Zehnder interferometers with only one AOFS, simultaneous sampling of two interferometric signals with the same clock system, and measuring and differentiating the frequencies of the two signals to obtain the exact Doppler frequency resulting from the moving object, the zero drift of heterodyne Doppler measurement systems caused by drift in the frequency shift of AOFS was completely eliminated. Furthermore, there were no concerns with the inconsistency of the clock systems of the photoelectric detection circuit and the AOFS driving circuit owing to the differential operation of the two interferometric signals. By using a custom-built experimental system and comparing with the measurement results of a conventional configuration, it was verified that the zero drift was successfully eliminated, and the displacement and velocity measurement accuracy reached 0.775 μm and 0.009 mm/s, respectively. In addition to the substantial improvement with regard to displacement and velocity measurements, it was also shown that the proposed system can withstand drastic temperature variation and thus has strong environmental adaptability.

Acknowledgments

This work was supported by the Open Foundation of the Key Laboratory of Photoelectric Testing and Instrument Technology of Shaanxi Province, Grant No. 2015SZSJ603; Xi'an Key Laboratory of Intelligent Detection and Perception, Grant No. 201805061ZD12CG45; Program for Fostering Talents of Xi'an Association for Science and

Technology, Grant No. 6; and the National Natural Science Foundation of China, Grant No. 61501363. In addition, we would like to thank Editage (www.editage.com) for English language editing. The authors declare that there are no conflicts of interest regarding the publication of this paper.

References

1. S. Shinohara et al., "Laser Doppler velocimeter using the self-mixing effect of a semiconductor laser diode," *Appl. Opt.* **25**(9), 1417–1419 (1986).
2. P. Castellini, M. Martarelli, and E. P. Tomasini, "Laser Doppler vibrometry: development of advanced solutions answering to technology's needs," *Mech. Syst. Signal Process.* **20**(6), 1265–1285 (2006).
3. E. T. Shimizu, "Directional discrimination in the self-mixing type laser Doppler velocimeter," *Appl. Opt.* **26**(21), 4541–4544 (1987).
4. P. Günther, T. Pfister, and J. Czarske, "Non-incremental interferometric displacement measurement using a laser Doppler sensor with phase coding," *Opt. Lasers Eng.* **49**(9–10), 1190–1193 (2011).
5. B. K. A. Ngoi et al., "Two-axis-scanning laser Doppler vibrometer for microstructure," *Opt. Commun.* **182**(1–3), 175–185 (2000).
6. S. Rothberg and J. Coupland, "The new laser Doppler accelerometer for shock and vibration measurement," *Opt. Lasers Eng.* **25**(4–5), 217–225 (1996).
7. A. R. Harland et al., "Application and assessment of laser Doppler velocimetry for underwater acoustic measurements," *J. Sound Vib.* **265**(3), 627–645 (2003).
8. L. Levin, D. Tzach, and J. Shamir, "Fiber optic velocity interferometer with very short coherence length light source," *Rev. Sci. Instrum.* **67**(4), 1434–1437 (1996).
9. L. Fabiny and A. D. Kersey, "Interferometric fiber-optic Doppler velocimeter with high-dynamic range," *IEEE Photonics Technol. Lett.* **9**(1), 79–81 (1997).
10. J. Weng et al., "New all-fiber velocimeter," *Rev. Sci. Instrum.* **76**(9), 093301 (2005).
11. S. Wu et al., "All-fiber configuration laser self-mixing Doppler velocimeter based on distributed feedback fiber laser," *Sensors* **16**(8), 1179 (2016).
12. J. E. Posada, J. A. Garciasouto, and J. Rubioserrano, "Multichannel optical-fibre heterodyne interferometer for ultrasound detection of partial discharges in power transformers," *Meas. Sci. Technol.* **24**(24), 094015 (2013).
13. C. J. Karlsson et al., "All-fiber multifunction continuous-wave coherent laser radar at 1.55 μm for range, speed, vibration, and wind measurements," *Appl. Opt.* **39**(21), 3716–3726 (2000).
14. A. T. Waz, P. R. Kaczmarek, and K. M. Abramski, "Laser-fibre vibrometry at 1550nm," *Meas. Sci. Technol.* **20**(10), 105301 (2009).
15. P. R. Kaczmarek et al., "Laser Doppler vibrometry with acoustooptic frequency shift," *Opt. Appl.* **34**(3), 373–384 (2004).
16. Y. Li et al., "Heterodyne laser Doppler vibrometers integrated on silicon-on-insulator based on serrodyne thermo-optic frequency shifters," *Appl. Opt.* **52**(10), 2145–2152 (2013).
17. W. Zhang et al., "Optical heterodyne micro-vibration measurement based on all-fiber acousto-optic frequency shifter," *Opt. Express* **23**(13), 17576–17583 (2015).
18. Y. Fu, M. Guo, and P. B. Phua, "Multipoint laser Doppler vibrometry with single detector: principles, implementations, and signal analyses," *Appl. Opt.* **50**(10), 1280–1288 (2011).
19. J. Shang et al., "Experimental study on minimum resolvable velocity for heterodyne laser Doppler vibrometry," *Chin. Opt. Lett.* **9**(8), 081201 (2011).
20. F. Li et al., "A fiber optic Doppler sensor and its application in debonding detection for composite structures," *Sensors* **10**(6), 5975–5993 (2010).
21. K. Shirai et al., "Highly spatially resolved velocity measurements of a turbulent channel flow by a fiber-optic heterodyne laser-Doppler velocity-profile sensor," *Exp. Fluids* **40**(3), 473–481 (2006).
22. J. Shang et al., "Laser Doppler vibrometer for real-time speech-signal acquirement," *Chin. Opt. Lett.* **7**(8), 732–733 (2009).
23. J. H. Shang et al., "Heterodyne laser Doppler vibrometer based on double acousto-optic frequency shifters," *Acta Photonica Sin.* **41**(10), 1149–1155 (2012).

Xiongxing Zhang received his BS degree in optoelectronic technology and science from Xidian University in 2002. He received his MS degree in computer science and technology from Xi'an Technological University in 2011. Currently, he is a lecturer at the School of Optoelectronic Engineering, Xi'an Technological University, Xi'an, China. His main research interests include optoelectrical measuring, computer graphics, and fiber-optic sensors.

Yanping Li received her BS degree in measurement and control technology and instrument from Xi'an Technological University in 2015. Currently, she is a MS candidate at the School of Optoelectronic Engineering, Xi'an Technological University, Xi'an, China. Her main research interests include optoelectrical measurement and fiber-optic sensors.

Wei Wang received his BS degree in mechanical design and manufacturing from Xi'an University of Architecture and Technology in 1996. He received his MS degree and PhD in mechanical manufacturing and automation from Northwestern Polytechnical University in 1999 and 2004, respectively. Currently, he is a professor at the School of Optoelectronic Engineering, Xi'an Technological University, Xi'an, China. His main research interests include optoelectrical measuring, industrial robotics, and fiber-optic sensors.

Haibin Chen received his BS degree from Harbin Institute of Technology in 2004, and his PhD from Zhejiang University in 2010. Currently, he is an associate professor at the School of Optoelectronic Engineering, Xi'an Technological University, Xi'an, China. His current research interests include fiber-optic sensors and micro/nano photonics.

Zilong Guo received his BS degree from Hebei University of Architecture, in 1999; his MS degree from China University of Petroleum; and his PhD from Xi'an Jiaotong University. Currently, he is an associate professor at the School of Optoelectronic Engineering, Xi'an Technological University, Xi'an, China. His current research interests include fiber-optic sensors and industrial robotics.

Yuxiang Yang received his PhD in biomedical engineering from Xi'an Jiaotong University in 2007. Currently, he is a full professor at the Department of Electronic Science and Technology in the Hunan Normal University, Changsha, China. His current research interests include biomedical signal detecting and processing, medical electronics, and intelligent instruments.